About EAS size spectra and primary energy spectra in the knee region

S.V. Ter-Antonyan*, L.S. Haroyan

Yerevan Physics Institute, Alikhanyan Brothers 2, Yerevan 375036, Armenia

Abstract

Based on the unified analyses of KASCADE, AKENO, EAS-TOP and ANI EAS size spectra, the approximations of energy spectra of different primary nuclei have been found. The calculations were carried out using the SIBYLL and QGSJET interaction models in 0.1-100 PeV primary energy range. The results point to existence of both rigidity-dependent steepening energy spectra at $R \simeq 200 - 400$ TV and an additional proton (neutron) component with differential energy spectrum $(6.1 \pm 0.7) \cdot 10^{-11}(E/E_k)^{-1.5}$ $(\text{m}^2 \cdot \text{s} \cdot \text{sr} \cdot \text{TeV})^{-1}$ before the knee $E_k = 2030 \pm 130$ TeV and with power index $\gamma_2 = -3.1 \pm 0.05$ after the knee.

---

*e-mail: samvel@jerewan1.yerphi.am

1 Introduction

High statistical accuracy in modern EAS experiments in the knee region encouraged the investigation of the fine structure of EAS size spectra. Although the origin of the knee is still a matter of debate, recently the series of publications [1] appeared, where the sharpness and the spectral structure in the knee region were interpreted by the contribution of heavy nuclei from a single local supernova. Along with this, the absolute differential EAS size spectra measured at different atmosphere depths and different zenith angles are not explained yet from the point of view of a single $A - A_{Air}$ interaction model and a single model of primary energy spectra and elemental composition. Such an attempt has been made in [2] based on the QGS interaction model and rigidity-dependent steepening primary energy spectra [3] for a description of vertical MSU, AKENO and Tien-Shan EAS size spectra. In the present work we worked out a formalism of the inverse problem solution - reconstruction of the primary energy spectrum and elemental composition based on the known EAS size spectra of KASCADE [4], AKENO [5], EAS-TOP [6] and ANI [7] measured at different zenith angles. The calculations were done in the frames of QGSJET [8] and SIBYLL [9] interaction models. As a primary spectrum we have tested the modified rigidity-dependent steepening primary energy spectra and the hypothesis of the additional component in the knee region [10, 11, 12, 13]. In this case the type of nucleus of the additional component was considering as unknown and determining by the best fit of the fine structure of EAS size spectra in the knee region.

2 EAS inverse problem

In general, the energy spectra $(\partial \Im_A / \partial E_0)$ of primary nuclei (A) and detectable EAS size spectra $(\partial I / \partial N_e^*)$ are related by the integral equation -

$$\frac{\partial I(E_e, \overline{\theta}, t)}{\partial N_e^*} = \sum_A \int_{E_{min}}^{\infty} \frac{\partial \Im_A}{\partial E_0} W_\theta(E_0, A, N_e^*, \overline{\theta}, t) dE_0 \tag{1}$$

where $E_0, A, \overline{\theta}$ are energy, nucleon number (1-59) and average zenith angle of primary nuclei, E_e is an energy threshold of detected EAS electrons, $N_e^*(E > E_e)$ is the estimation value of EAS size obtained by the electron lateral distribution function. Here, by the EAS size $(N_e(E > 0))$ we mean the total number of EAS electrons at given observation level (t). The kern (W_θ) of integral equation (1) is determined as

$$W_\theta \equiv \frac{1}{\Delta_\theta} \int_{\theta_1}^{\theta_2} \int_0^{\infty} \frac{\partial \Omega(E_0, A, \theta, t)}{\partial N_e} P_\theta \frac{\partial \Psi(N_e)}{\partial N_e^*} \sin\theta d\theta dN_e$$

where $\partial \Omega / \partial N_e$ is an EAS size spectrum at the observation level (t) for given E_0, A, θ parameters of a primary nucleus and depends on $A - A_{Air}$ interaction model; $\Delta_\theta = \cos\theta_1 - \cos\theta_2$;

$$P_\theta \equiv P(Ne, E_0, A, \theta) = \frac{1}{X \cdot Y} \int\int D(N_e, E_0, A, \theta, x, y) dx dy$$

2

is a probability to detect an EAS by scintillation array at EAS core coordinates $|x| < X/2$, $|y| < Y/2$ and to obtain the estimations of EAS parameters (N_e^*, s - shower age, x^*, y^* - shower core location) with given accuracies; $\partial\Psi/\partial N_e^*$ is a distribution of $N_e^*(N_e, s, x, y)$ for given EAS size (N_e).

One may achieve significant simplification of equation (1) providing the following conditions during experiments:

a) selection of EAS cores in a range where $P_\theta \equiv 1$,

b) the log-Gaussian form of the measuring error ($\partial\Psi/\partial N_e^*$) with an average value $\ln(N_e \cdot \delta)$ and a RMSD σ_N, where δ involves all transfer factors (an energy threshold of detected EAS electrons, γ and μ contributions) and slightly depends on E_0 and A,

c) transformation (standardization) of the measured EAS size spectra to the EAS size spectra at observation level

$$\frac{\partial I(0, \overline{\theta}, t)}{\partial N_e} \simeq \eta \frac{\partial I(E_e, \overline{\theta}, t)}{\partial N_e^*},$$

where $\eta = \delta^{(\gamma_e - 1)} \exp\{(\gamma_e - 1)^2 \sigma_N^2 / 2\}$ and γ_e is the EAS size power index,

d) consideration of either all-particle primary energy spectrum $\partial\Im_\Sigma/\partial E_0$ with effective nucleus $A_{eff}(E_0)$ or energy spectra of primary nuclei ($\partial\Im_{A_\xi}/\partial E_0$) gathered in a limited number of groups ($\xi = 1, \ldots \xi_{\max}$) as unknown functions.

(a-d) conditions make EAS data of different experiments more comparable and equation (1) converts to the form

$$\frac{\partial I(0, \overline{\theta}, t)}{\partial N_e} = \eta \int_{E_{min}}^{\infty} \frac{\partial\Im_\Sigma}{\partial E_0} \frac{\partial\Omega(E_0, A_{eff}(E_0), \overline{\theta}, t)}{\partial N_e} dE_0 \tag{2}$$

or

$$\frac{\partial I(0, \overline{\theta}, t)}{\partial N_e} = \eta \sum_{\xi=1}^{\xi_{\max}} \int_{E_{min}}^{\infty} \frac{\partial\Im_{A_\xi}}{\partial E_0} \frac{\partial\Omega(E_0, \overline{A}_\xi, \overline{\theta}, t)}{\partial N_e} dE_0 \tag{3}$$

However, even in this form the determination of primary energy spectra by measured EAS size spectra and solution of integral equations (2,3) in general is unsolvable problem. At the same time, using the a priori information about energy spectra of primary nuclei ($\partial\Im_{A_\xi}/\partial E_0$) and the EAS size spectra $\partial I/\partial N_e^* \equiv f_{i,j}(N_{e,i}^*, \overline{\theta}_j, t)$ measured in $i = 1, \ldots m$ size intervals and $j = 1, \ldots n$ zenith angular intervals, one may transform the inverse problem into χ^2-minimization problem

$$\min\{\chi^2\} \equiv \min\left\{ \sum_i^m \sum_j^n \frac{(f_{i,j} - F_{i,j})^2}{\sigma_f^2 + \sigma_F^2} \right\} \tag{4}$$

with unknown (free) spectral parameters. Here $F_{i,j} \equiv F(N_{e,i}^*, \overline{\theta}_j, t)$ are the expected EAS size spectra determined at the right hands of equations (1-3) and σ_f, σ_F are the uncertainties (RMSD) of measured ($f_{i,j}$) and expected ($F_{i,j}$) shower size spectra.

One may also unify the data of different experiments applying minimization χ_U^2 with re-normalized EAS size spectra

$$\min\{\chi_U^2\} \equiv \min\left\{\chi^2\left(\frac{f_{i,j,k}}{\sum_i \sum_j f_{i,j,k}}, \frac{F_{i,j,k}}{\sum_i \sum_j F_{i,j,k}}\right)\right\} \tag{5}$$

where index $k = 1, \ldots l$ determines the observation levels (t) of experiments. Expression (5) offers an advantage for experiments where the values of methodical shift (δ) and measuring error (σ_N) are unknown or known with insufficient accuracy.

The energy spectra of primary nuclei are preferable to determine (a priori) in the following generalized form

$$\frac{\partial \Im_A}{\partial E_0} \simeq \beta \cdot \Phi_A \cdot E_0^{-\gamma_1(A)} \cdot \left(1 + \left(\frac{E_0}{E_{knee}(A)}\right)^\epsilon\right)^{(\gamma_1(A)-\gamma_2)/\epsilon} \tag{6}$$

Unknown (free) spectral parameters in approximation (6) are β, $E_{knee}(A)$ (so called "knee" of energy spectrum of A nucleus), γ_1 and γ_2 (spectral asymptotic slopes before and after knee), ϵ (sharpness parameter of knee, $1 \leq \epsilon \leq 10$). The values of Φ_A and $\gamma_1(A)$ parameters are known from approximations of balloon and satellite data [14] at $A \equiv 1, 4, \ldots 59$ and $E_0 \simeq 1 - 10^3$ TeV. Parameter $\beta \simeq 1$ determines the normalization of spectra (6) in $10^2 - 10^5$ TeV energy range.

Thus, minimizing χ^2- functions (4,5) on the basis of measured values of $\partial I(\overline{\theta}_{i,k})/\partial N_{ej,k}$ and corresponding expected EAS size spectra (2,3) at given m zenith angular intervals, n EAS size intervals and l experiments one may evaluate the parameters of the primary spectrum (6). Evidently, the accuracies of solutions for spectral parameters strongly depend on the number of measured intervals $(m \cdot n \cdot l)$, statistical errors and correctness of $\partial \Omega(E_0, A, \theta, t)/\partial N_e$ determination in the framework of a given interaction model.

3 Results

Here, the parametric solutions of the EAS inverse problem are obtained on the basis of KASCADE [4] ($t = 1020$ g/cm^2), AKENO [5] (910 g/cm^2), EAS-TOP [6] (810 g/cm^2) and ANI [7] (700 g/cm^2) published EAS size spectra. These experiments were carried out at different observation levels and were chosen for two reasons: satisfaction of (a-c) conditions from the section (2) and a high statistical accuracy of presented data (especially KASCADE experiment). Unfortunately, during the standardization of EAS size spectra (condition (c)) the value of η parameter is not always known with proper accuracy, which is the main reason of discrepancy in the results of different experiments. In our calculations we included η in the list of unknown spectral parameters and determined by the minimization of functional (4). The problem does not exist if the minimization of re-normalized EAS size spectra is unified, since the linear parameters $(\eta_k \cdot \beta)$ are canceled out from the functional (5).

The differential EAS size spectra $\partial \Omega(E_0, A, \theta, t)/\partial N_e$ for given $E_0 \equiv 0.032, 0.1, \ldots, 100$ PeV,

$A \equiv 1, 4, 12, 16, 28, 56$, $t \equiv 0.5, 0.6, \ldots, 1$ Kg/cm^2, $\cos\theta \equiv 0.8, 0.9, 1$ were calculated using COR-SIKA562(NKG) EAS simulation code [15] at QGSJET [8] and SIBYLL [9] interaction models. Intermediate values are calculated using 4-dimensional log-linear interpolations. The estimations of errors of the expected EAS size spectra $\partial\Omega/\partial N_e$ at fixed E_0, A, θ, t parameters did not exceed $3 - 5\%$.

The basic results of minimizations (4,5) at a given number (ν) of unknown spectral parameters and the values of χ^2/q (or χ^2_U/q_u for unified data), are presented in Tables 1-4, where $q = mn - \nu - 1$ and $q_u = \sum_k (mn)_k - \nu - 1$ are corresponding degrees of freedom. The upper (lower) rows of each experiment in Tables 1 and 4 correspond to parameters obtained by the QGSJET (SIBYLL) interaction model.

3.1 Test of rigidity-dependent energy spectra

Table 1 contains the approximation values of spectral parameters at rigidity-dependent approach [3]

$$E_{knee}(A) = R \cdot Z \tag{7}$$

where Z is a charge of A nucleus and R is a parameter of magnetic rigidity (or a critical (cutoff) energy in more modern model [13, 14]). The results were obtained by minimizations (4,5) applying (6,7). The magnitudes of $\gamma_1(A)$ for all nuclei were taken from [14]. The number of unknown (free) parameters is equal to $\nu = 4$ and corresponding solutions at two interaction models are presented in Table 1.

The stability of solutions (or the steep of χ^2 global minimum) of minimizations (4,5) is seen from obtained errors. So, it is seen that the χ^2 minimum for AKENO data does not depend on the ε sharpness parameter at SIBYLL and partly at QGSJET interaction models.

The obtained slopes of primary energy spectra after knee agree with the same calculations [2] performed by QGS model and exceed well known expected values $(3 - 3.1)$ in the $\sim 10^{17}$ eV energy range [14]. Such a steep of primary spectra after the knee is a result of (γ_2, R) correlations in (4-7). In case of $R \simeq 2000$ TeV the $E_k(Fe) \simeq 5.2 \cdot 10^4$ TeV and the primary energy spectra in the large interval $(E_k(H) - E_k(Fe))$ at fixed $\gamma_1(A_\xi)$ can be conformed with corresponding EAS size spectra provided abnormally steep slope $(\gamma_2 \simeq 3.4 - 3.5)$ after the knee.

The results of expected EAS size spectra in comparison with corresponding experimental data are shown in Fig. 1 (the thin solid lines by QGSJET model, the thin dashed lines by SIBYLL model). Despite the satisfactory agreement $(\chi^2 \sim 1)$ of EAS size spectra with predictions of rigidity-dependent steepening spectra (6,7) and QGSJET interaction model the form (fine structure) of the measured EAS size spectra in the knee region differs from the form of corresponding expected spectra. It is worth mentioning that the difference is formally small and does not exceed several

5

Experiment	R [TV]	γ_2	ϵ	$\eta \cdot \beta$	χ^2/q
KASCADE	2390±190	3.46±0.12	2.2±0.3	1.05±0.08	1.3
$m \cdot n = 24 \cdot 5$	2310±220	3.45±0.12	1.8±0.2	0.69±0.05	3.0
AKENO	3150±120	3.50±0.14	10±7.0	1.98±0.06	2.2
$m \cdot n = 20 \cdot 3$	2820±110	3.50±0.31	10±?	1.48±0.04	3.1
EAS-TOP	1450±120	3.35±0.11	2.3±0.5	1.43±0.03	1.2
$m \cdot n = 24 \cdot 5$	1540±205	3.35±0.20	1.4±0.3	1.15±0.04	0.5
ANI	2030±245	3.47±0.18	2.1±0.5	1.07±0.02	0.8
$m \cdot n = 23 \cdot 3$	2230±320	3.49±0.23	1.9±0.4	0.87±0.02	1.0
Unified data	2610±710	3.47±0.23	1.3±0.2	-	1.7
$\sum m \cdot n = 369$	3000±650	3.49±0.30	1.2±0.1	-	2.3

Table 1: Rigidity (R), slope (γ_2), "sharpness" (ϵ), shift ($\eta \cdot \beta$) and corresponding χ^2/q values obtained by approximations of EAS size spectra at QGSJET (upper rows) and SIBYLL (lower rows) interaction models and rigidity-dependent assumption (7).

Model	$E_k(H)$[TeV]	$E_k(He,Li)$	$E_k(Be\text{-}Na)$	$E_k(Mg\text{-}Cl)$	$E_k(Ar\text{-}Ni)$	χ_U^2/q_u
QGSJET	3070±160	790±70	5550±60	6310±50	9020±170	1.7
SIBYLL	3150±90	610±30	6060±65	6970±40	9780±90	2.3

Table 2: Spectral parameters $E_{knee}(A)$ $[TeV]$ for different groups of primary nuclei and different interaction models. The results obtained by unified analyses of EAS data at $\gamma_2 = 3.1$ and $\epsilon = 4$.

percents in precise KASCADE data.

As a next step, we attempted to test the rigidity-dependent approximation (7) directly. The knee-energies $E_k(A_\xi)$ were chosen as unknown (free) parameters in the approximations of EAS data (4-7), where $\xi = 1, \ldots \xi_{max}$. However, the stable solutions for free parameters were obtained only at unified minimization (5), fixed values $\gamma_1(A_\xi), \gamma_2, \varepsilon$ and number of nuclear groups $\xi_{max} \leq 5$. In Table 2 the values of spectral parameters $E_{knee}(A_\xi)$ obtained by minimization of χ_U^2 (5) for 5 groups of primary nuclei (H), (He, Li), $(Be - Na)$, $(Mg - Cl)$, $(Ar - Ni)$ at given values of $\gamma_2 = 3.1$, $\epsilon = 4.0$ and $\nu = 5$ are presented. It is seen, that approach (7) is performed only for nuclei with $A > 1$ and $R \simeq 400$ TV or (7) is valid for all nuclei at $R \simeq 400$ TV but there is an additional proton flux with $E_{knee}^{(p)} \simeq 3000$ TeV which shifts the knee value of the total proton energy spectrum.

The following testing of the rigidity-dependent approach (7) is based on the investigation of the

Model	γ_1	γ_2	E_k [TeV]	a	b_1	b_2	χ_U^2/q_u
QGSJET	2.72±0.01	3.05±0.03	2180±110	1.71±0.14	-0.30±0.13	0.86±0.12	1.5
SIBYLL	2.79±0.02	3.09±0.02	3680±230	10.5±1.00	-0.28±0.20	4.24±0.61	1.4
R=600TV	2.66±0.01	3.09±0.01	3400±200	7.0±0.5	0.25±0.15	3.0±0.5	1.2

Table 3: Parameters of all-particle energy spectrum obtained by unified EAS data (the first and second rows). The last row corresponds to results of extrapolation of fits [14] taking into account the assumptions (6,7) at $R = 600$ TV.

all-particle energy spectrum. Toward this end the fits of primary energy spectra $d\Im_A/dE_0$ for different nuclei ($A = 1, \ldots 59$) known from [14] were extrapolated up to $E_A = 10^5$ TeV energies taking into account (6,7) at $R \simeq 600$ TeV [13]. The obtained expected all-particle energy spectrum $dI_\Sigma/dE_0 = \sum_A d\Im_A/dE_0$ was approximated by expression similar to (6) at five free parameters $(\Phi_\Sigma, \gamma_1, \gamma_2, E_k, \varepsilon)$. The average values of primary nuclei ($\exp(\overline{\ln A})$) obtained from extrapolations of spectra [14] were approximated by step function

$$A_{eff}(E_0) = a + b \cdot \ln\left(\frac{E_0}{E_k}\right) \tag{8}$$

where $b = b_1$ at $E_0 < E_k$ and $b = b_2$ at $E_0 > E_k$. The results of these approximations are presented in a last row of Table 3 . The value of sharpness parameter was equal to $\varepsilon = 1 \pm 0.1$.

The first and second rows of Table 3 content the parameters of the all-particle energy spectra $(\partial\Im_\Sigma/\partial E_0)$, which were obtained by minimization χ_U^2 (expressions 2,5-7) of unified EAS size data at $\nu = 6$ and $\varepsilon = 1$. The approximation (8) has been used for $A_{eff}(E_0)$ which is at the right hand of expression (2). It is necessary to note that the solutions for a, b_1, b_2 parameters can be obtained only by re-normalized EAS size spectra (5) because of the strong correlation between a linear parameter η and an effective nucleus A_{eff}.

It is seen from Table 3 that the model of rigidity-dependent energy spectra predicts the increase ($b_1 > 0$, third row of Table 3) of the mean nucleus with energy, whereas the presented analysis of EAS data points out a decrease of A_{eff} with energy ($b_1 < 0$, first two rows of Table 3) in the energy range of $E_0 < E_k$. It is obvious, that despite $\overline{A}$ could not be exactly equal to A_{eff}, at least their dependence on energy must be the same.

The results of recent precise experiments DICE [17] and CASA-BLANKA [18] also point out to the decrease of $\overline{\ln A}$ with energy at $E_0 < E_k$. This dependence of A_{eff} and $\overline{\ln A}$ on energy might be explained by the contribution of an additional light component in a primary nuclei flux.

From the above analyses follows that rigidity-dependent steepening energy spectra in combination with QGSJET or SIBYLL interaction model can not explain the obtained results of the fine

structure of EAS size spectra [4, 5, 6, 7] in the knee region (Table 1 and Fig. 1), the large values of knee $E_k(H)$ for Hydrogen component (Table 2) and dependence of the effective nucleus $A_{eff}(E_0)$ on primary energy before the knee (Table 3). In this connection we have carried on the search of more adequate model of primary energy spectra and elemental composition.

3.2 Test of additional component

Based on predictions [10, 11, 12, 13] the primary energy spectra in approximation (6) have been added by a new (polar cap [13]) component $\partial\Im_{Add}/\partial E_0$ with power energy spectrum

$$\frac{\partial\Im_{Add}}{\partial E_0} = \Phi^{(p)}\big(E_k^{(p)}\big)^{\gamma_1^{(p)}}\left(\frac{E_0}{E_k^{(p)}}\right)^{-\gamma^{(p)}} \tag{9}$$

where $\gamma^{(p)} = \gamma_1^{(p)}$ at $E_0 < E_k^{(p)}$ and $\gamma^{(p)} = \gamma_2$ at $E_0 > E_k^{(p)}$.

New spectral parameters $\Phi^{(p)}, \gamma^{(p)}, E_k^{(p)}$ and nucleon number $A^{(p)}$ of the additional component are considered as unknown and determined together with parameters of rigidity-dependent energy spectra (6,7) by minimization of χ^2 and χ_U^2 (4,5) at $\nu = 7$. The results of expected EAS size spectra for each experiment (KASCADE, AKENO, EAS-TOP and ANI) taking into account contribution of additional component (9) are shown in Fig. 1 (the thick solid lines by QGSJET model and the thick dashed lines by SIBYLL model). It is seen that the additional component with high accuracy (2-5% for KASCADE and ANI data) describes the fine structure of EAS size spectra in the knee region. The values of slopes of additional component before the knee turned out to be $\gamma_1^{(p)} \simeq 1.5\pm_{0.2}^{0.6}$. The nucleon number $(A^{(p)})$ of this component with high reliability did not exceed of $A^{(p)} = 1$ for most of experiments especially at QGSJET interaction model (except from AKENO $(A^{(p)} \simeq 56)$). The unified analyses of all experiments at QGSJET and SIBYLL interaction models also gave a proton or neutron $(A^{(p)} = 1)$ composition of the additional component. The values of other spectral parameters at $\gamma_1^{(p)} = 1.5$ and $A^{(p)} = 1$ are included in Table 4.

The obtained result disagrees with [1] where the alike component consists of several heavy nuclei. However, our result is based on the high accuracy of the coincidence ($\sim 2 - 3\%$ for KASCADE data) of expected and measured EAS size spectra by both χ^2 criterion and the overlapping of fine structure of spectra.

The comparison of parameters γ_2 from Tables 1,4 shows that spectral slopes after the knee from Table 4 roughly overlap with the expected slope $(3 - 3.1)$ well known from $N_e \gg 10^7$ EAS data. This can be explained the fact that the spectral brake of summary proton component $(E_k^{(p)} \simeq 2 \cdot 10^3$ TeV) is closer to the iron component $(E_k(Fe) \simeq 10^4$ TeV) at $R \simeq 400$ TV.

The coexistence of rigidity-dependent primary energy spectra and additional proton flux with spectral parameters $E_k^{(p)} \simeq 2000$ TeV, $\gamma_1^{(p)} \simeq 1.5$, $\gamma_2^{(p)} = \gamma_2 \simeq 3.1$ explains also the shifted value of the knee $E_k(H)$ in Table 2 and the decrease of $A_{eff}(E_0)$ at $E_0 < E_k$ (see section 3.1).

Although the additional component does not contribute to shower sizes below or above the knee

Experiment	R [TV]	$E_k^{(p)}$[TeV]	$\Phi^{(p)} \cdot 10^6$	γ_2	$\eta \cdot \beta$	χ^2/q
KASCADE	195±30	1960±150	11.6±1.0	3.15±0.04	1.11±0.02	0.8
	150±20	1820±85	12.8±0.6	3.14±0.03	0.74±0.07	2.3
AKENO	290±180	4240±370	4.04±0.10	3.25±0.05	2.60±0.07	2.0
	290±210	3860±310	4.59±0.16	3.24±0.03	1.86±0.02	3.0
EAS-TOP	390±150	1960±30	6.08±0.10	3.16±0.02	1.43±0.01	1.1
	150±95	2110±130	4.37±0.50	3.11±0.04	1.41±0.04	0.3
ANI	240±130	2060±145	6.80±0.80	3.09±0.03	1.14±0.07	0.5
	160±85	2050±130	6.38±0.70	3.05±0.02	1.02±0.02	0.8
Unified data	390±30	2030±130	5.55±0.60	3.09±0.01	-	1.6
$\sum m \cdot n = 369$	322±15	2150±100	4.92±0.35	3.08±0.01	-	2.2

Table 4: Spectral parameters taking into account the contribution of additional proton component.

significantly , it is essential for the reproducing of the sharp knee of EAS size spectra. This idea is taken from [13] and is confirmed here.

The final all-particle energy spectrum $(\partial I/\partial E_0)$ obtained by unified EAS size data at QGSJET interaction model

$$\frac{\partial I}{\partial E_0} = \beta\Big(\sum_A \frac{\partial \Im_A}{\partial E_0} + \frac{\partial \Im_{Add}}{\partial E_0}\Big)$$

and corresponding energy spectra $(\partial \Im_A/\partial E_0)$ of 6 nuclear groups with additional component $(\partial \Im_{Add}/\partial E_0)$ at normalization $\beta = 1$ [14] are presented in Fig. 2. The solid (dashed) line is the all-particle energy spectrum obtained by unified (only KASCADE) EAS size spectra. Dotted lines are the energy spectra of different primary components obtained by unified EAS data. Symbols in Fig. 2 are the data from DICE [17], CASA-BLANKA [18] arrays and reviews [14, 16].
The numerical values of all-particle energy spectrum (solid line in Fig. 2), corresponding error, spectrum of additional proton component and average nucleus versus primary energy are presented in Table 5.

Conclusion

High statistical accuracy of experiments KASCADE, EAS-TOP, AKENO and ANI allowed to obtain approximations of primary energy spectra and elemental composition with accuracy $\sim 15\%$ in the knee region. Along with this, KASCADE and ANI EAS size spectra at $\theta < 37^0$ are described with the accuracy of $\sim 2-5\%$ in a whole measurement interval.

E_0 (TeV)	$\partial I/\partial E_0$ $(m^2 \cdot sr \cdot s \cdot$ $\cdot TeV)^{-1}$	$\Delta(\partial I/\partial E_0)$ $\pm(m^2 \cdot sr \cdot$ $\cdot s \cdot TeV)^{-1}$	$\partial \Im_{Add}/\partial E_0$ $(m^2 \cdot sr \cdot s \cdot$ $\cdot TeV)^{-1}$	$\overline{\ln A}$
0.200E+03	0.174E-06	0.15E-07	0.196E-08	1.71
0.250E+03	0.964E-07	0.87E-08	0.140E-08	1.72
0.312E+03	0.534E-07	0.50E-08	0.100E-08	1.73
0.391E+03	0.296E-07	0.31E-08	0.719E-09	1.73
0.488E+03	0.161E-07	0.18E-08	0.514E-09	1.76
0.610E+03	0.884E-08	0.10E-08	0.368E-09	1.78
0.763E+03	0.486E-08	0.56E-09	0.263E-09	1.79
0.954E+03	0.260E-08	0.33E-09	0.188E-09	1.81
0.119E+04	0.140E-08	0.18E-09	0.135E-09	1.82
0.149E+04	0.762E-09	0.10E-09	0.965E-10	1.81
0.186E+04	0.418E-09	0.57E-10	0.681E-10	1.79
0.233E+04	0.224E-09	0.32E-10	0.395E-10	1.81
0.291E+04	0.117E-09	0.18E-10	0.199E-10	1.88
0.364E+04	0.609E-10	0.10E-10	0.100E-10	1.94
0.455E+04	0.316E-10	0.58E-11	0.502E-11	2.00
0.568E+04	0.163E-10	0.33E-11	0.252E-11	2.05
0.711E+04	0.843E-11	0.18E-11	0.126E-11	2.11
0.888E+04	0.435E-11	0.10E-11	0.634E-12	2.16
0.111E+05	0.222E-11	0.57E-12	0.318E-12	2.19
0.217E+05	0.280E-12	0.77E-13	0.402E-13	2.19
0.827E+05	0.448E-14	0.14E-14	0.642E-15	2.19

Table 5: Expected all-particle flux, error, flux of additional component and average nucleus at different primary energies.

Obtained results show the evidence of QGSJET interaction model at least in $10^5 - 10^7$ TeV energy range, rigidity-dependent steepening primary energy spectra at $R \simeq 200 - 400$ TV and existence of the additional proton (or neutron) component with spectral power index $\gamma_1^{(p)} \simeq 1.5 \pm_{0.2}^{0.6}$ before the knee $E_k^{(p)} \simeq 2030$ TeV. The contribution of the additional proton (neutron) component in all-particle energy spectrum turned out to be $20 \pm 5\%$ at primary energy $E_0 = E_k^{(p)}$.

Acknowledgements

References

[1] A.D. Erlykin, A.W. Wolfendale, Astropart. Phys. 7 (1997) 1 //Astropart. Phys. 7 (1997) 203 // Astropart. Phys. 8 (1998) 265.

[2] G.B. Khristiansen, Yu.A. Fomin, N.N. Kalmykov et al., Proc. 24th ICRC, **2**, Rome (1995) 772.

[3] B. Peters, Nuovo Cimento (Suppl.) **14**, (1959) 436 // Nuovo Cimento **22**, (1961) 800.

[4] R. Classtetter et al. (KASCADE Collaboration), Nucl.Phys. B (Proc.Suppl.) 75A (1999) 238.

[5] M. Nagano, T. Hara et al., J.Phys.G:Nucl.Phys. **10** (1984) 1295 // ICR-Report 16-84-5, Tokyo (1984) 30 p.

[6] M. Aglietta et al. (EAS-TOP Collaboration), INFN/AE-98/21 (1998) 15 p.// M. Aglietta et al., Astropart. Phys. (10) 1 (1999) 1.

[7] A. Chilingaryan et al., Proc. 26th ICRC, Salt Lake City, **1** (1999) 240.

[8] N.N. Kalmykov, S.S. Ostapchenko, Yad. Fiz. **56** (1993) 105 // Phys.At.Nucl. **56** (3) (1993) 346.

[9] R.S. Fletcher, T.K. Gaisser, P. Lipari, T. Stanev, Phys.Rev. D **50** (1994) 5710 // J. Engel, T.K. Gaisser, P. Lipari, T. Stanev, Phys.Rev.D. **46** (1992) 5013.

[10] J. Kempa et al., J.Phys.A: Math.,Gen. **7** (1974) 1213.

[11] J. Linsley, Proc. 18th ICRC, Bangalore (1983) **12**, 135.

[12] T.K. Gaisser and T.Stanev, Proc. 22nd ICRC, Dublin (1991).

[13] T. Stanev, P.L. Biermann, T.K. Gaisser, Astron. Astrophys. 274 (1993) 902 // P.L. Biermann, Preprint MPIfR, Bonn, No 700 (1996) 6.

[14] B. Wiebel-Sooth and P. Biermann, Preprint Max-Planck Inst. für Radioastr., Bonn, No.772, (1998) 50 p.

[15] D. Heck, J. Knapp, J.N. Capdevielle, G. Schatz, T. Thouw, Forschungszentrum Karlsruhe Report, FZKA 6019 (1998) 90 p.

[16] S. Petrera, Proc. 24th ICRC, Rapp. Papers, Rome (1995) 737. **2**, 101.

[17] S.P. Swordy, D.B. Kieda, Astropart. Phys. 13 (2000) 137.

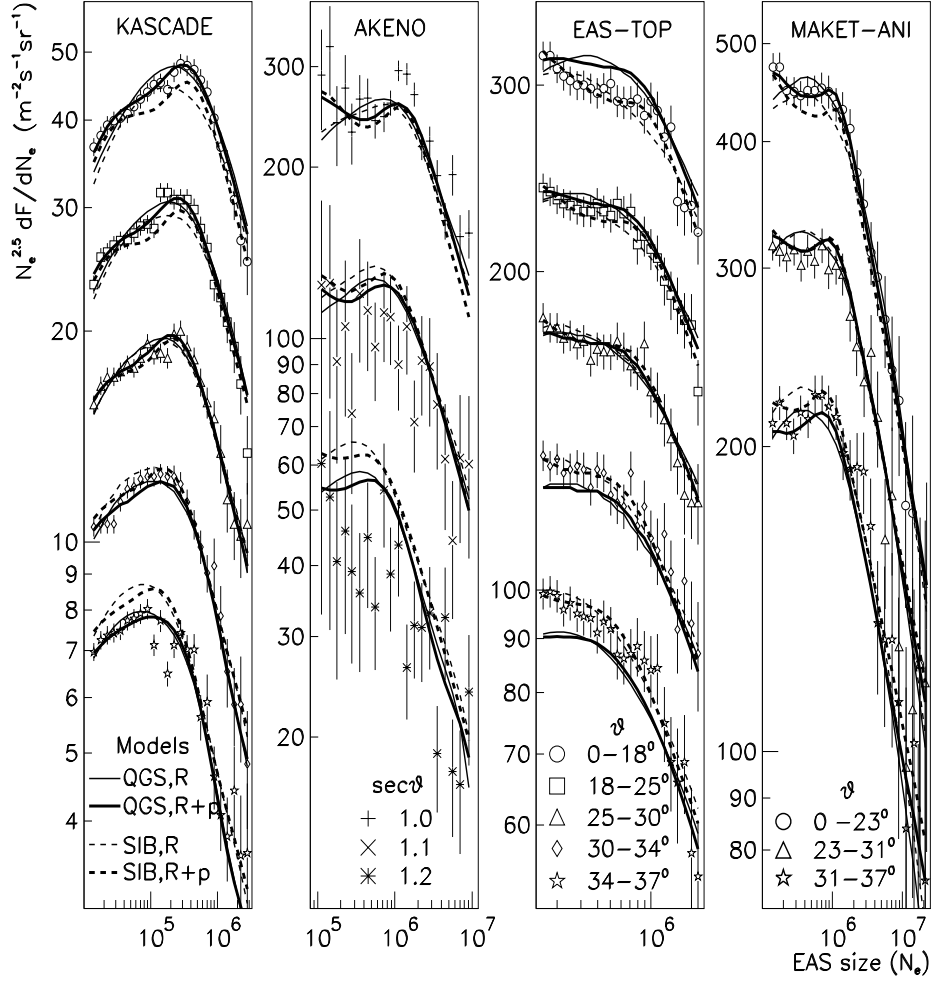[18] J.W. Fowler, L.F. Fortson et al., Preprint, arXiv:astro-ph/0003190(2000).

Figure 1: KASCADE, AKENO, EAS-TOP and ANI EAS size spectra (symbols). The thin (thick) lines correspond to predictions via rigidity-dependent steepening primary spectra (with the additional proton component). The solid and dashed lines correspond to the QGSJET and SIBYLL interaction models respectively.
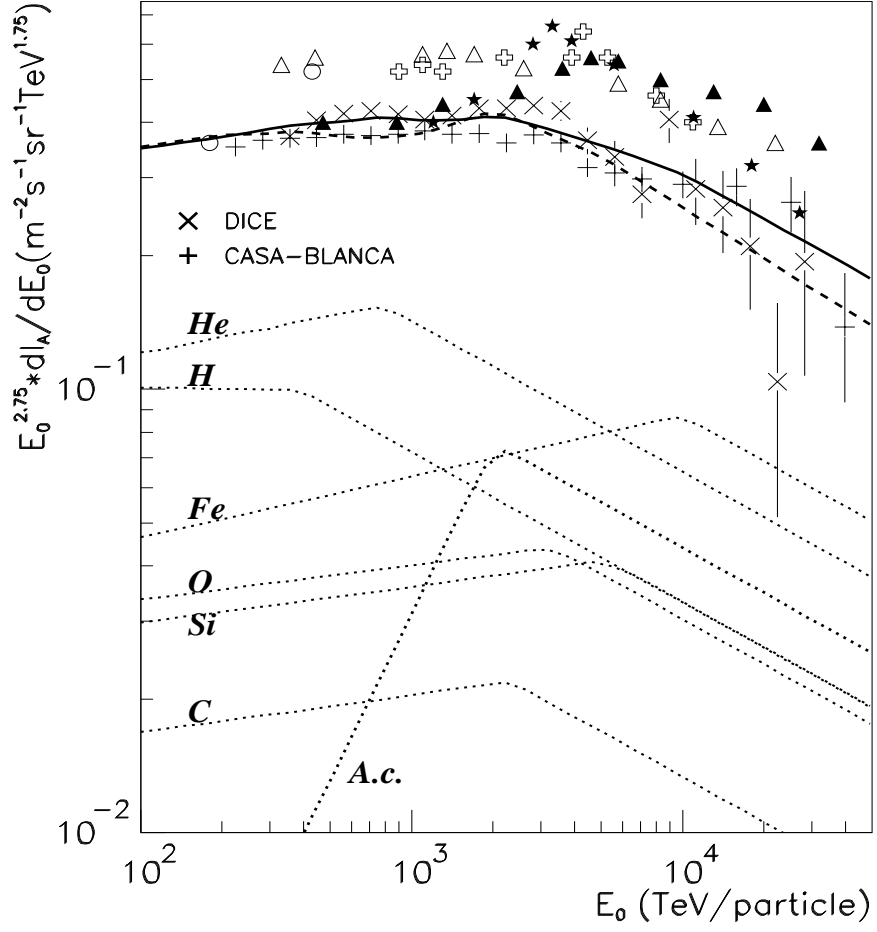
13

Figure 2: Primary energy spectra and elemental composition. The solid (dashed) line is the all-particle energy spectrum obtained by unified (only KASCADE) EAS data. The dotted lines are the energy spectra of different nuclear groups. The A.c. dotted line is the energy spectrum of additional proton component. The symbols are the data from [17, 18] and reviews [14, 16].